Journal of Thermal Analysis (1985) 813–830

SPECTROSCOPIC AND THERMOANALYTICAL CHARACTERIZATION OF STANDARD SUBSTANCES FOR THE IDENTIFICATION OF REACTION PRODUCTS ON IRON ELECTRODES

G. Nauer, P. Strecha, N. Brinda-Konopik and *G. Liptay**

INSTITUTE FOR PHYSICAL CHEMISTRY, UNIVERSITY OF VIENNA,
1090 WIEN, WÄHRINGERSTRASSE 42, AUSTRIA
*DEPARTMENT OF INORGANIC CHEMISTRY, TECHNICAL UNIVERSITY OF BUDAPEST,
1521 BUDAPEST, GELLÉRT TÉR 4, HUNGARY

(Received February 12, 1985)

The in situ spectroscopic investigation of electrochemical, and especially corrosion processes in iron requires well-characterized reference substances. It has been found that the application of spectroscopic methods alone is not sufficient for the detection of impurities in certain phases. Thermoanalytical methods have therefore additionally been used to detect impurities and to optimize the preparation methods. Infrared and Raman spectra and thermoanalytical data on α-FeOOH, β-FeOOH, γ-FeOOH, δ-FeOOH and on amorphous iron(III) hydroxide sol are reported.

The in situ investigation of the electrochemical behaviour of iron by means of FTIR (Fourier transform infrared) and Raman spectroscopy requires the spectra of possible reaction products for identification. The iron oxyhydroxides α-FeOOH, β-FeOOH, γ-FeOOH and δ-FeOOH and an amorphous iron(III) hydroxide sol were prepared and were examined by X-ray techniques, infrared and Raman spectroscopy, and thermoanalytical methods.

Experimental

Methods of preparation

Various methods of preparation for the above-mentioned substances, some of which occur in nature, are described in the available literature [1–11].

On the basis of comprehensive but preliminary investigations concerning the preparation of α, γ and δ-FeOOH, those methods were avoided which involve the

John Wiley & Sons, Limited, Chichester
Akadémiai Kiadó, Budapest

use of chloride in any preparation step. The reason for this is that the differential thermal analysis of substances prepared in this way displayed exothermic peaks also found in the chloride-stabilized phase (Cl, F, $OH)_2Fe_8(O, OH)_{16}$, "β-FeOOH" [12].

As we were mainly interested in single phases containing only Fe, O and H, it was necessary to assume an impurity in the products prepared in the presence of chloride, in spite of the agreement not only of the IR and Raman spectra, but also of the X-ray data, with published data. Alternative preparation methods were therefore followed whenever possible.

It was never possible to obtain completely water-free products, for these substances adsorb water when exposed to air (detected by the characteristic IR band of the H—O—H bending vibration at 1620 cm^{-1}). The X-ray purity was examined for all products.

α-FeOOH goethite

In the light of the previously mentioned facts, the method of Atkinson *et al.* [8] is appropriate. 20.2 g (0.05 mol) $Fe(NO_3)_3 \cdot 9H_2O$ was dissolved in distilled water in a polyethylene flask. 10 ml 2.5 *M* NaOH was added immediately (final volume 100 ml). Local precipitations dissolved after shaking; the pH ranged between 1 and 1.5. The resulting sol of iron hydroxide was aged at room temperature for 48 hr and then poured into 100 ml ca. 1.3 *M* NaOH and preserved in an incubator at 60° for 120 hr (shaking at 12-hr intervals). When the crystallization was finished, the product was washed to neutrality by repeatedly suspending, centrifugating and decanting. It was finally stored as a dilute aqueous suspension. For the subsequent investigations it was filtered through a glass filter crucible and dried under oil-pump vacuum at room temperature. Final product: reddish light-brown powder.

β-FeOOH (akaganite)

preparation according to Weiser *et al.* [11]. 0.2 mol (54 g) $FeCl_3 \cdot 6H_2O$ was dissolved in 2000 ml deionized water and heated in a thermostat from 25° to 80° over a period of 8 hr. A turbidity due to the precipitation of β-FeOOH was first observed at 60°. After sedimentation overnight, the product was washed twice with deionized water and five times with weak ammonia solution, and dried at 110° for 17 hr. Final product: yellowish-brown powder.

γ-FeOOH (lepidocrocite)

Preparation according to Baudisch and Hartung [7] using the reaction

$$FeCl_2 + 4\ C_5H_5N \rightarrow Fe(C_5H_5N)_4Cl_2 \xrightarrow{\text{air}} \gamma\text{-FeOOH}$$

50.5 ml pyridine was degassed under nitrogen, then mixed with 13.6 ml concentrated $FeCl_2$ solution and left overnight. The resulting yellow sediment was filtered off and dried over $CaCl_2$. 19.7 g tetrapyridine iron(II) chloride was dissolved in 1000 ml water, and a vigorous current of air was blown into the solution for 45 minutes during stirring. The product was washed first with acetone and then with ether, and finally dried under vacuum at room temperature. Final product: orange powder.

δ-FeOOH

Preparation according to Glemser and Gwinner [10]. 5 g $FeSO_4 \cdot 7H_2O$ was dissolved in 40 ml distilled water. A solution of 50 g NaOH in 60 ml water was added during cooling and stirring. The resulting mixture, containing a dark-blue/green flaky sediment, was cooled to approximately 30°. Then, 15 ml 15% H_2O_2 solution was added for oxidation. The fine brown sediment was washed to neutrality by centrifugating and decanting, and dried at 45° for 3 days. Final product: dark-brown ferromagnetic powder.

$Fe(OH)_3$

Preparation according to Glemser and Rieck [4]. 50 g $Fe(NO_3)_3 \cdot 9H_2O$ dissolved in 1000 ml distilled water was added to 1000 ml NH_3 solution (6%) during stirring. The sediment was allowed to deposit overnight. The overlying solution was aspirated off, and the sediment was mixed and stirred with distilled water several times and then filtered through a rough paper filter until wash-water reacted neutrally. The product was dried at 50° for 2 days. Final product: dark-brown powder.

Infrared spectroscopic investigations

The infrared spectroscopic investigations were carried out on a BRUKER IFS 113 V FTIR (Fourier transform infrared spectrometer. The radiation source was a globe, and for each spectral range special detectors were used.

The samples were investigated as KBr pills (0.5 to 20 mg substance and 300 mg KBr) in transmission, and for comparison as powder, pressed on Ge or KRS5 crystals in ATR (attenuated total reflection) mode. The positions of the absorption bands can be seen from Table 1.

The infrared spectra of the examined substances can be divided into three interesting regions:

1) 3600 to ca. 3000 cm^{-1}: Region of the OH stretching vibration, $\nu(OH)$.

The absorption maximum is shifted by hydrogen-bonding to smaller wavenumbers (compared to the valence vibration of free OH^- ions at 3630 cm^{-1}) [4, 13, 14], and is often significantly broadened.

2) 1200 to 600 cm^{-1}: Region of the Fe—O—H bending vibrations and the Fe—O stretching vibrations [14, 15].

Table 1 Infrared frequencies of the Fe-oxihydroxides, stated in wavenumbers (cm^{-1})
Intensity statements: ss very strong
s strong
m medium
w weak
vw very weak
sh shoulder

	α-FeOOH		β-FeOOH		γ-FeOOH		δ-FeOOH		$Fe(OH)_3$	
1)			ss	3480					m	3500–2500
	s	3155			s	3100	s	3150		
2)					m	1155	m	1130		
					m	1020				
							m	915		
	s	890	sh	875					w	890
	s	790	w	800	s	740	s	795	w	795
			s	700						
	s	640	w	620						
3)	sh	455			ss	480	ss	460		
	ss	400	ss	425						
					ss	360	ss	335		
	s	270			ss	270				

3) 600 to 200 cm^{-1}: This region includes absorptions [16] caused by the overlapping of lattice vibrations with molecular frequencies. Fe—O stretching vibrations can also absorb down to around 350 cm^{-1} [17].

Bands appearing at around 1620 cm^{-1} can be ascribed to the bending vibration of H—O—H. No references to substance-specific absorption bands for this spectral range could be found in the literature.

In these spectra it is difficult to distinguish the Fe—O stretching vibrations from the Fe—O—H bending frequencies, because they appear in practically the same spectral region. Glemser and Hartert [14, 15] were able to establish certain relations through comparisons with the spectra of isomorphic metal oxyhydroxides (see Table 1).

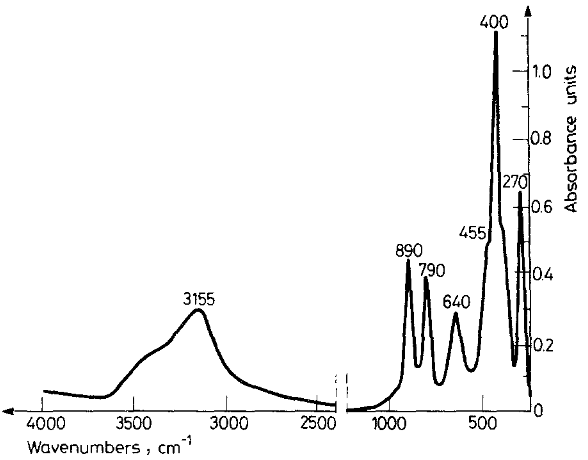

Fig. 1 IR spectrum of α-FeOOH

α-FeOOH (see Fig. 1)

The absorption band ν(OH) has its maximum at 3155 cm^{-1}. The sharp, distinct and intense pair of bands at 890 and 790 cm^{-1} can be ascribed to the Fe—O—H bending vibration [14, 15]; consequently, the bands at 640 cm^{-1} can be ascribed to a Fe—O stretching vibration. Further, absorption bands appear at 455 (shoulder), 400 and 270 cm^{-1}.

β-FeOOH (see Fig. 2)

The absorption maximum of the ν(OH) vibration is at 3480 cm^{-1}. In the second spectral range, absorptions appear at 875 (shoulder), 800, 700 and 620 cm^{-1}, and in the lower region at 425 cm^{-1}.

γ-FeOOH (see Fig. 3)

The ν(OH) absorption maximum is at 3100 cm^{-1}. In the characteristic second spectral range, there is a band at 1155 cm^{-1}; the band of the Fe—O—H bending vibration lies at 1020 cm^{-1} [15]; the band at 740 cm^{-1} can be ascribed to an Fe—O valence vibration. In the area of low wavenumbers, there are bands at 480, 360 and 270 cm^{-1} (overlapping of lattice and molecular frequencies).

δ-FeOOH (see Fig. 4)

The ν(OH) stretching vibration absorbs maximally at 3150 cm^{-1}. Three characteristic, distinct bands appear in the second spectral range, at 1130, 915 and

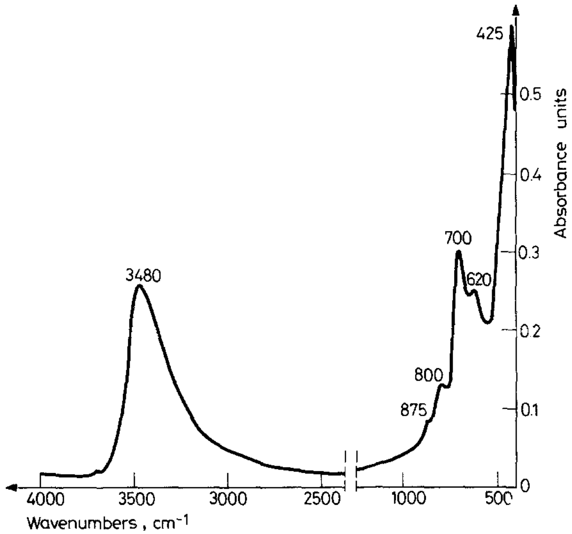

Fig. 2 IR spectrum of β-FeOOH

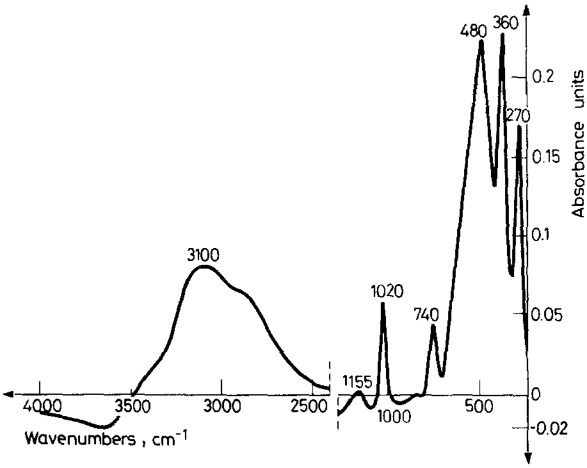

Fig. 3 IR spectrum of γ-FeOOH

795 cm^{-1}. Nevertheless, they have not yet been assigned to specific vibration modes. In the lower region of the overlapping frequencies, rather broad absorptions are observed at 460 and 335 cm^{-1}.

$Fe(OH)_3$ (see Fig. 5)

It must be stated that the nature of the amorphous sol "$Fe(OH)_3$" is controversial [4, 18, 19], and that the selected formula is one of many proposed in the available

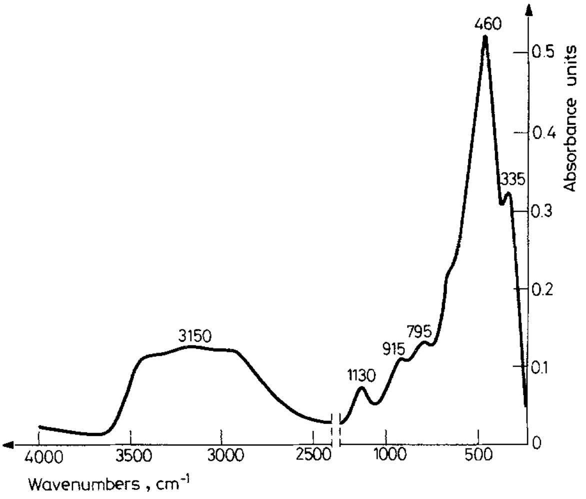

Fig. 4 IR spectrum of δ-FeOOH

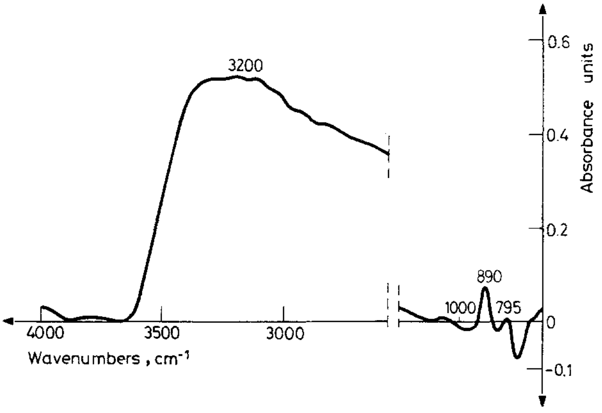

Fig. 5 IR spectrum of $Fe(OH)_3$

literature. A knowledge of the infrared spectra of the various modifications of iron oxyhydroxide could shed light on the question of the nature of amorphous iron(III) hydroxide. On the one hand, a relatively intense, broad band appears in the region of ν(OH). On the other hand, we can observe relatively sharp, but weak absorptions in the region of the Fe—O stretching and/or the Fe—O—H bending frequencies (890 and 785 cm^{-1}), respectively. The presence of a true hydroxide is thereby confirmed. In addition to this, however, there is a relatively distinct absorption in the region of the HOH bending vibration (1620 cm^{-1}), which indicates a certain amount of (adsorbent or occluded) water.

These observations suggested a mixed character of pure oxide hydrate and pure hydroxide. According to Glemser and Rieck [4], the infrared spectra of different "$Fe(OH)_3$" gel preparations vary greatly with changing ageing and dehydration conditions.

It is further noteworthy that "$Fe(OH)_3$" absorbs continuously in the region below 600 cm^{-1}. In other words, no specific absorptions can be measured, and thus there is no evidence relation to lattice vibrations. This situation is brought about by the amorphous character of the examined materials, which is confirmed by the complete absence of any X-ray reflexions. The very limited crystallinity is confirmed by the weakly structured thermoanalytical effects see below.

Short discussion of the Raman spectra

There are certain difficulties in the recording of Raman spectra: the iron oxyhydroxides are thermally unstable during the measurements, and the relatively low sensitivity of this method leads to difficulties in the exact interpretation of the spectra, for it is not always possible to distinguish between a shift of background and a real Raman band.

Table 2 Raman frequencies of the Fe-oxihydroxides, stated in wavenumbers (cm^{-1})
Intensity statements: ss very strong
s strong
m medium
w weak
vw very weak

α-FeOOH		β-FeOOH		γ-FeOOH		δ-FeOOH
				ss	252	
ss	299					
		m	330			
ss	397			m	380	
		m	415			
m	479					
vw	550			w	526	
				w	650	663 broad
vw	685					
		ss	745			
vw	1003					
				s	1307	

Further, the signal intensity was negatively influenced by the partially "amorphous" state of the samples (e.g. with $Fe(OH)_3$ we could not obtain any significant Raman bands).

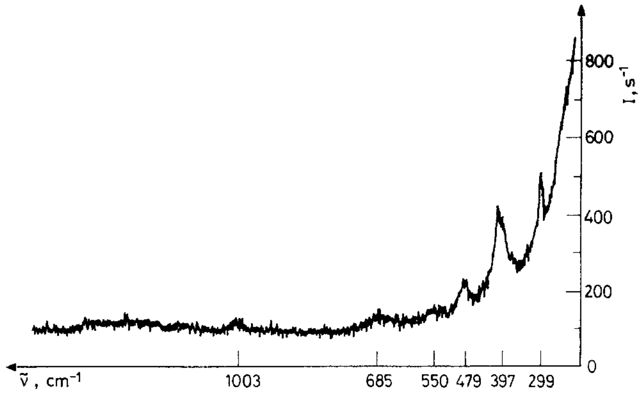

Fig. 6 Raman spectrum of α-FeOOH

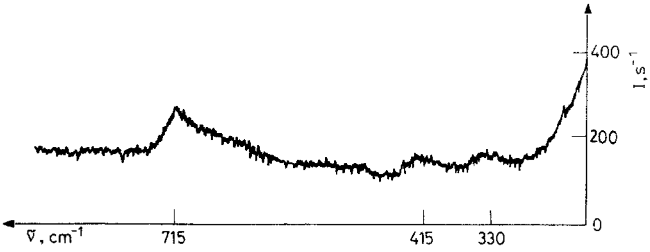

Fig. 7 Raman spectrum of β-FeOOH

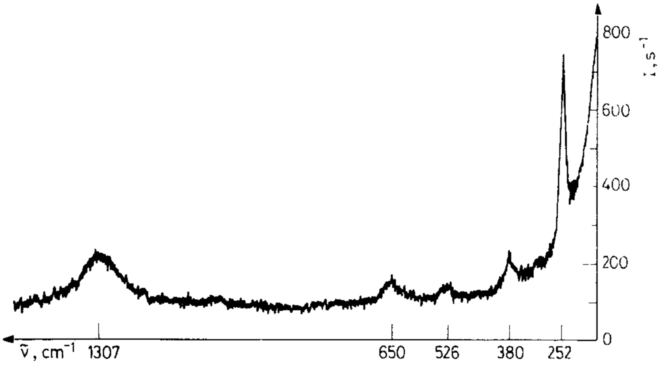

Fig. 8 Raman spectrum of γ-FeOOH

The samples were investigated as powder, or pressed together with KBr (ratio 1 : 1) in pills. The excitation laser wavelength was 514.5 nm.

The bands recorded are listed in Table 2.

Excellent Raman spectra can be obtained from α-FeOOH and γ-FeOOH (see Figs 6 and 8) as already reported by Keiser et al. [9] and Thibeau et al. [20]. Both substances give intense Raman lines in the range between 250 and 400 cm^{-1}; the bands at 400 cm^{-1} might be assigned to the Fe—O stretching vibrations.

Both β- and δ-FeOOH (see Figs 7 and 9) gave less distinct spectra, with broad bands at 745 cm^{-1} (β-FeOOH) and 663 cm^{-1} (δ-FeOOH) in the range of the Fe—O stretching vibrations. Additional weak bands occur for β-FeOOH at 330 and 415 cm^{-1}. Keiser et al. [9] report further Raman bands of δ-FeOOH at 299, 397 and 550 cm^{-1}. These bands, which we could not find for δ-FeOOH, are identical to those of the strongest vibrations of α-FeOOH (presumably due to impurities in the reference sample).

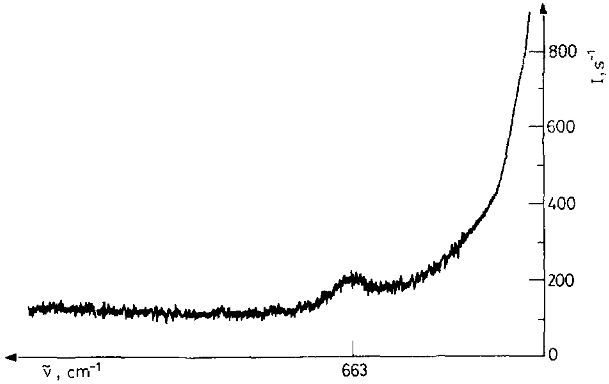

Fig. 9 Raman spectrum of δ-FeOOH

Because of the strongly marked Raman spectra of α-FeOOH and γ-FeOOH, it is possible to investigate both substances in situ, i.e. with the sample surface in contact with an electrolyte solution or simply water. This seems especially important for the investigation of different iron corrosion problems.

Thermoanalytical data

The thermoanalytical investigations were carried out on a Paulik–Paulik–Erdey derivatograph. The heating rate was 10 degree/minute, and the sample amount was 100 mg. The reference substance for DTA analysis was α-Al$_2$O$_3$.

With β-FeOOH, additional investigations were carried out in varying atmospheres, and one test was run with simultaneous recording of the mass spectrum of the evolved gases.

α-FeOOH (see Fig. 10)

Water-free products do not exist. The physically bonded water is released at 50 to 120°, and the chemically bonded water at 300 to 400°. The end-product is α-Fe_2O_3 [2].

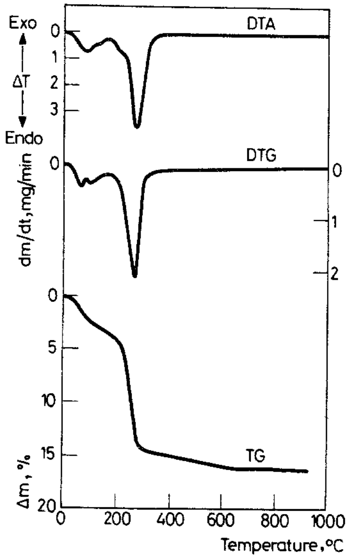

Fig. 10 Thermoanalytical curves of α-FeOOH

Our product:

The DTA curve shows endothermic peaks at 120° and 280°, and a step at 225°. Physically adsorbed water is released at 120° (steep slope in the TG curve and a minimum in the DTG curve). The release of water during the reaction

$$2\ \alpha\text{-FeOOH} \rightarrow \alpha\text{-Fe}_2\text{O}_3 + \text{H}_2\text{O}$$

occurs at 250° (step) and 280°. The loss in mass during continued heating is minimal at 320°. The minimum in the DTG curve is at 280°.

Discussion

Wieghardt and Lange [2] report that α-FeOOH decomposes in two steps, at 235° and 290°, which correspond to the respective minima in the DTG curves. These values are in good agreement with our results, if the slow heating rate described in the literature (1 degree/minute) is taken into account. The differences in position and form of the two peaks can be explained, according to Derie et al. [21], by variations in the specific surface of the samples.

Babcan and Kristin [22] report still another exothermic peak in the DTA curve, at approximately 270°. This peak cannot be assigned to the transition from α-FeOOH to α-Fe_2O_3. The transition possibly passes through an instable intermediate stage, which might be γ-Fe_2O_3. There is no documentation on of this in the literature.

The end-product of all thermoanalyses is α-Fe_2O_3 [2, 22].

Spinzi and Niculescu [23] find endothermic transitions at 200° and 298° in all topochemically produced mixtures (heating rate 10 degree/minute). The peak at 300° is assigned to the dehydration of goethite. A small peak at lower temperatures is perhaps connected with structural water (water diffusion) or is due to structural transformation of the α-FeOOH into amorphous α-Fe_2O_3.

β-FeOOH (see Fig. 11)

The existence of β-FeOOH is controversial. The first studies were performed by Boehm [24], Weiser and Milligan [25], and Kratky and Nowotny [26]. Keller [12], Babcan and Kristin [22], Mackenzie [27] and Mackay [28] carried out the first thermoanalytical studies.

Keller [12] established a new formula for "β-FeOOH": $(Cl, F, OH)_2Fe_8(O, OH)_{16}$. Akaganeite, which is found in nature, conforms to this formula without Cl and F, but can nevertheless not be produced synthetically.

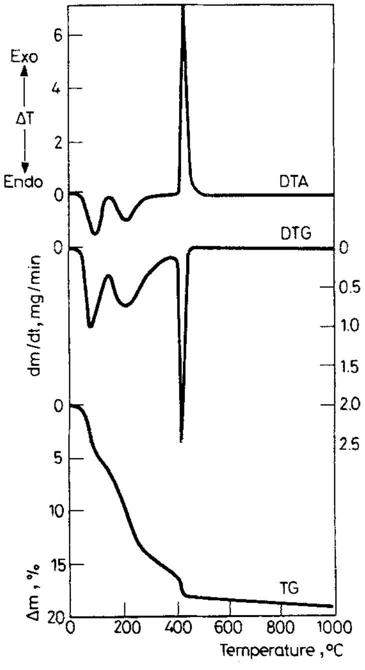

Fig. 11 Thermoanalytical curves of β-FeOOH

Our product:

The X-ray analysis is in agreement with the values for "β-FeOOH" cited in the literature [26].

A small endothermic peak appears at 90° (at 70° resp.) in the DTA curve. At 205°, there is a large peak. The DTG curve shows a minimum in this region, and the TG displays a sharp, downward slope equivalent to a 12.5% loss in mass. A sharp exochtermic peak appears at 395° in the DTA curve; a 2% mass loss occurs simultaneously. The mass does not vary on further heating.

Discussion

As previously mentioned, Keller [12] denies the existence of β-FeOOH. All compounds produced until now conform to the formula which he proposes: $(Cl, F, OH)_2Fe_8(O, OH)_{16}$.

Varying DTA and DTG curves were obtained, depending on the chloride or fluoride content and on the crystallinity of the samples. The exothermic peaks appear only in the case of substances with pronounced lattice defects, or amorphous products such as amorphous iron hydroxide gels.

It seems clear that the first endothermic reaction is the release of moisture, and the second endothermic reaction, at approximately 200° to 230° is the release of OH groups [12, 22, 29].

The strong exothermic peak at 390° in the DTA curve corresponds to the release of protons and chloride ions as HCl, which we were able to prove directly by mass spectrometry. This effect is significantly less pronounced in a nitrogen atmosphere. Paterson et al. [30] interpret this in terms of completely different decomposition mechanisms in oxygen and nitrogen atmospheres. Additionally, they observed some transport of iron in nitrogen atmospheres, which fact is also reported by Gonzales-Calbet and Alario Franco [31].

In agreement with the above, Ishikawa and Inouye [32] report a peak at 370° in the EGD (evolved gas detection) curve. In contrast to the peaks obtained during water release, they could not eliminated this peak by the insertion of a cooling trap (−20°).

γ-FeOOH (see Fig. 12)

γ-FeOOH occurs as lepidocrocite in nature. Giovanoli and Brütsch [33, 34] reported on the production of pure phases and comprehensive thermochemical studies of the kinetics and mechanism of dehydration.

Our product

Endothermic peaks appear at 80° in the DTA curve (in a non-dried product there is a shoulder at 80° and a peak at 130°) and at 255 to 260°. There is an exothermic peak at 430°. There is also a small peak at 640° in some cases.

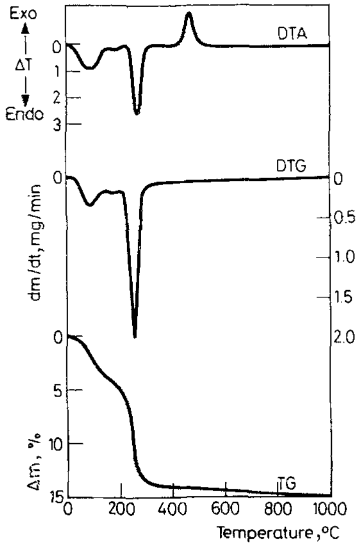

Fig. 12 Thermoanalytical curves of γ-FeOOH

The release of physically adsorbed water takes place between 80° and 130°. Dehydration according to the formula

$$2\,\gamma\text{-FeOOH} \rightarrow \gamma\text{-Fe}_2\text{O}_3 + \text{H}_2\text{O}$$

occurs at 260°. The exothermic peak at 430° corresponds to the transformation of γ-Fe_2O_3 into α-Fe_2O_3. The endothermic peak at 640° is due to a change in the magnetic properties. This means the Curie-point of Fe_2O_3 but the thermal effect does not always appear in the DTA curve as the enthalpic change is very small. It can be observed for only a few other FeOOH modifications.

Discussion

With the exception of the position of the release of chemically bonded water, the observed values agree with those cited in the literature [2]. The dehydrations of the other products always occur at temperatures approximately 40° higher, in the range

300 to 360°. In contrast, Arora et al. [35] specify approximately 250 as the temperature of transformation of γ-FeOOH to γ-Fe_2O_3.

The exothermic reaction can be interpreted as the transformation of cubic γ-Fe_2O_3 into pseudohexagonal α-Fe_2O_3. It is evident from the DTG and TG curves that no loss of mass occurs above 300. Therefore, transformation can only take place within the lattice. The slight differences in peak temperature for the exothermic transformation can be ascribed to variations in the crystallinity and particle size of the products. Different experimental conditions, such as varying heating rates, also contribute to these differences.

δ-FeOOH (see Fig. 13)

Studies by Wieghardt and Lange [2] and Spinzi and Niculescu [23] are to be found in the literature.

Our product:

Physically adsorbed water is released at 80°. Additional water is given up continuously until 155°. A step appears at 70° in the DTG curve. According to the DTA curve, the release of chemically bonded water takes place in two endothermic reactions, at 250° and 300°.

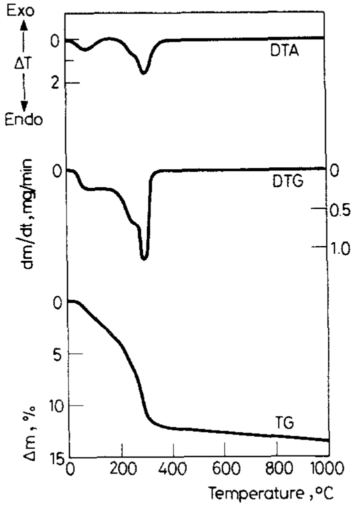

Fig. 13 Thermoanalytical curves of δ-FeOOH

There are corresponding minima in the DTG curve. The TG curve decreases only linearly up to approximately 280°, corresponding to a 12% relative mass loss. There is no further loss in mass above 300°.

Discussion

The results are in accordance with those published in the literature: water is released continuously over a wide temperature range, but two reactions apparently occur (different activation energies). The end-product of the thermal decomposition is α-Fe_2O_3 directly, i.e. without the transitional compound (γ-Fe_2O_3). This well-crystallized end-product does not undergo any further transformations.

$Fe(OH)_3$ (see Fig. 14)

Our product:

Physically adsorbed water is released continuously up to 150° (cf. the broad peaks in the DTA and DTG curves). A weak endothermic loss of water occurs at 250° (shoulder in the DTG curve, minimum in the DTA curve).

Further, an exothermic peak without change in mass is seen at 420° in the DTA curve.

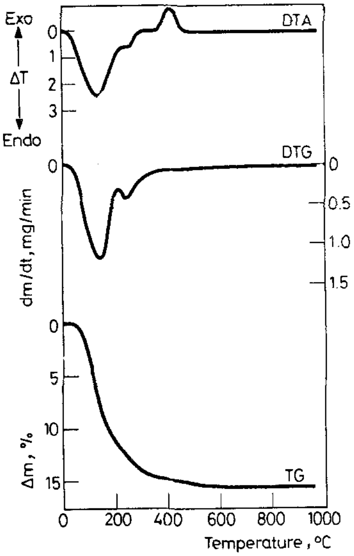

Fig. 14 Thermoanalytical curves of $Fe(OH)_3$

Discussion

Limited quantities of chemically water (250°) are present in addition to physically bonded water. Similarly as in the case of γ-FeOOH, an exothermic transformation of the structure occurs at 420°. This transformation can be considered to be recrystallization of the amorphous product.

Conclusion

It has been shown that it is necessary to employ several different methods for the characterization of reference substances. The thermoanalytical investigation methods are an excellent supplement to the spectroscopic methods, as they provide useful information about the composition with relatively little sacrifice of time. The effective single-phase character of the prepared substances could be proved in some instances only by thermal analysis. The different results obtained in the cited publications can be explained satisfactorily by considerable differences in the experimental conditions.

* * *

We gratefully acknowledge the financial support given by the "Fonds zur Förderung der wissenschaftlichen Forschung" of Austria. We also thank Prof. A. Otto (Düsseldorf) and Prof. H. Kuzmany (Wien) for measuring the Raman spectra; thanks are also due to Prof. R. Kellner (Wien) for his kind permission to use the FTIR equipment.

References

1 G. Brauer, Handbuch der Präparativen Anorganischen Chemie Bd 3, Stuttgart 1981, S. 1647.
2 G. Wieghardt and D. Lange, die Technik 29 (1974) 590.
3 O. Glemser, Z. Anorg. Allg. Chem., 240 (1939) 263.
4 O. Glemser and G. Rieck, Z. Anorg. Allg. Chem., 297 (1958) 181.
5 O. Glemser, Z. Elektrochem., 44 (1938) 346.
6 K. J. Gallagher and D. N. Phillips, Trans. Faraday Soc., 64 (1968) 785.
7 O. Baudisch and W. H. Hartung, Inorg. Synth., Vol. 1, 185.
8 R. J. Atkinson, A. M. Posner and J. P. Quirk, J. Inorg. Nucl. Chem., 30 (1968) 2371.
9 J. T. Keiser, C. W. Brown, and R. H. Heidersbach, Int. Laboratory, 7/8 (1982) 12.
10 O. Glemser and Gwinner, Z. Anorg. Allg. Chem., 240 (1939) 161.
11 H. B. Weiser, W. O. Milligan and E. L. Cook, Inorg. Synth., Vol. II, 215 (1946).
12 P. Keller N. Jb. Miner. Abh., 113 Heft 1 (1970) 29.
13 H. Siebert, Anwendungen der Schwingungsspektroskopie in der anorganischen Chemie, in: Allgemeine und anorganische Chemie in Einzeldarstellungen, Bd. VII, Hrsg. M. Beckegoehring, Berlin, 1966.
14 E. Hartert and O. Glemser, Naturwissensch., 40 (1953) 552.
15 E. Hartert and O. Glemser, Z. Elektrochem., 60 (1956) 746.
16 W. Bruegel, Einführung in die Ultrarot-Spektroskopie, 2. Auf., Darmstadt, 1957.
17 P. Tarte and G. Nizet, Spectrochim. Acta, 20 (1946) 305.
18 O. Glemser, Nature, 183 (1959) 1476.
19 O. Glemser, Nature, 183 (1959) 943.
20 R. S. Thibeau, C. W. Brown and R. H. Heidersbach, Appl. Spectrosc., 32 (1978) 532.
21 R. Derie, M. Ghodsi and C. Calvi-Roche, J. Thermal Anal., 9 (1976) 435.
22 J. Babcan and J. Kristin, J. Thermal Anal., 3 (1971) 307.

23 A. Spinzi and I. V. Niculescu, Revue Romaine de Chimie, 20, 3 (1975) 387.
24 J. Böhm, Z. Anorg. Allg. Chem., 149 (1925) 203.
25 H. B. Weiser and W. O. Milligan, J. Am. Chem. Soc., 39 (1935) 25.
26 O. Kratky and H. Nowotny, Z. Kristallographie, 100 (1938) 256.
27 R. C. Mackenzie, Miner. Soc. London, 1957.
28 A. L. Mackay, Mineral. Mag., 32 (1960) 545.
29 P. Keller, Werkstoffe und Korrosion, 20 (1969) 102.
30 E. Patterson, R. Swaffield and D. R. Clark, Thermochim. Acta, 54 (1982) 201.
31 J. M. Gonzalez-Calbet and M. A. Alario Franco, Thermochim. Acta, 58 (1982) 45.
32 T. Ishikawa and K. Inouye, J. Thermal Anal., 10 (1976) 399.
33 R. Giovanoli and R. Brütsch, Chimia, 28 (1974) 188.
34 R. Giovanoli and R. Brütsch, Thermochim. Acta, 13 (1975) 15.
35 B. R. Arora, N. K. Mandal, R. L. Chowdhury, N. C. Ganguli and S. N. Sen, Technology, 9 (1972) 143.

Zusammenfassung — Die in situ-Untersuchung von elektrochemischen und speziell von Korrosionsprozessen an Eisen mit spektroskopischen Methoden erfordert gut charakterisierte Standardsubstanzen. Es zeigte sich, daß die spektroskopische Charakterisierung allein nicht ausreicht, um Verunreinigungen in definierten Phasen zu erkennen. Deshalb wurden zusätzlich thermoanalytische Untersuchungsmethoden zur Auffindung von unreinen Substanzen und zur Optimierung der Präparationsmethoden angewandt. Es werden IR- und Ramanspektroskopische sowie thermoanalytische Daten von α-, β-, γ- und δ-FeOOH sowie eines amorphen Eisen(III) hydroxidsols berichtet.

Резюме — Спектроскопическое исследование in situ электрохимических и, особенно, коррозийных процессов в железе, требует хорошо идентифицированных реперных веществ. Найдено, что применение только спектроскопических методов недостаточно для обнаружения примесей в определенных фазах. В связи с этим, для обнаружения примесей и оптимизации методов получения, дополнительно были использованы термоаналитические методы. Приведены ИК спектри и спектри комбинационного рассеяния, а также термоаналитические данные для α-FeOOH, β-FeOOH, γ-FeOOH, δ-FeOOH и золя аморфной гидроокиси трехвалентного железа.